Diagnostic Ability of Macular Nerve Fiber Layer Thickness Using New Segmentation Software in Glaucoma Suspects

Jose M. Martinez-de-la-Casa,[1] Pilar Cifuentes-Canorea,[1] Clara Berrozpe,[1] Marina Sastre,[1] Vicente Polo,[2] Javier Moreno-Montañes,[3] and Julian Garcia-Feijoo[1]

[1]Servicio de Oftalmologia, Hospital Clinico San Carlos; Departamento de Oftalmologia, Facultad de Medicina, Universidad Complutense de Madrid; and Instituto de Investigacion Sanitaria del Hospital Clinico San Carlos (IdISSC), Madrid, Spain
[2]Servicio de Oftalmología, Hospital Miguel Servet, Zaragoza, Spain
[3]Servicio de Oftalmología, Clinica Universitaria de Navarra, Pamplona, Spain

Correspondence: Jose M. Martinez-de-la-Casa, Hospital Clinico San Carlos, Martin Lagos sn, 28040 Madrid, Spain;
martinezcasa@ya.com.

Submitted: August 19, 2014
Accepted: November 4, 2014

Citation: Martinez-de-la-Casa JM, Cifuentes-Canorea P, Berrozpe C, et al. Diagnostic ability of macular nerve fiber layer thickness using new segmentation software in glaucoma suspects. *Invest Ophthalmol Vis Sci.* 2014;55:8343–8348. DOI DOI:10.1167/iovs.14-15501

Purpose. To assess the capacity of internal retinal layer thickness measurements made at the macula using new spectral-domain optical coherence tomography (OCT) software to distinguish between healthy subjects and those with suspected glaucoma. The diagnostic performance of such measurements also was compared with that of conventional peripapillary retinal nerve fiber layer (RNFL) thickness measurements.

Methods. The study included 38 subjects with suspected glaucoma and 38 age-matched healthy subjects. In one randomly selected eye of each participant, thickness measurements at the level of the macula were made of the nerve fiber layer (mRNFL), the ganglion cell layer (GCL), and the ganglion cell complex (GCC; GCL + internal plexiform layer) through automated OCT segmentation. Peripapillary RNFL thickness (pRNFL) also was determined using the conventional scan.

Results. As the only variable showing intergroup variation, mRNFL in the glaucoma suspects was significantly thinner in the quadrants inner inferior ($P = 0.003$), inner temporal ($P = 0.010$), and outer inferior ($P = 0.017$). The variable best able to discriminate between the two groups was inner inferior mRNFL thickness, as indicated by an area below the receiver operating characteristic (ROC) curve of 0.742.

Conclusions. Macular RNFL thickness measurements showed an improved diagnostic capacity over the other variables examined to distinguish between healthy subjects and glaucoma suspects.

Keywords: glaucoma, optical coherence tomography, macula, retinal nerve fiber layer, ganglion cell

Glaucoma is a disease of multifactorial etiology characterized by a gradual loss of retinal ganglion cells (RGCs) produced by damage to their axons inside the optic nerve head.[1,2] If left untreated, glaucoma can lead to irreversible vision loss and is one of the leading causes of blindness in developed countries.[3]

Diagnostic tools for glaucoma have sought to detect the disease at its earliest stages, with the objective of delaying disease progression to avoid, in the measure possible, vision loss and its effects on the quality of life of affected patients.[4]

Traditionally, stereo- and red-free photographs have been used to examine the state of the optic nerve and retinal nerve fiber layer (RNFL). Although this method is still considered the gold standard, the interpretation of photographs has a subjective component and shows high intra- and interobserver variability.[5,6]

The recent introduction of automated image analysis systems has meant that researchers and clinicians can objectively and quantitatively assess the changes that lead to glaucoma. Optical coherence tomography (OCT), initially temporal domain and more recently spectral, or Fourier, domain, achieves a quantitative analysis of the morphology of the papilla and RNFL. These techniques have shown a high capacity to diagnose glaucoma by comparing measurements in the eye examined with normative databases.

The high proportion of RGCs present at the level of the macula led Zeimer et al.[7] to propose macular thickness as an early indicator of glaucomatous damage. However, in subsequent studies, its diagnostic capacity proved limited.[8–10] The new segmentation software designed for spectral-domain OCT enables the independent measurement of each of the retinal layers most affected by glaucoma at the macular level: the nerve fiber layer, the ganglion cell layer (GCL), and the internal plexiform layer, which, respectively, contain the ganglion cell axons, cell bodies, and dendrites.

This study was designed to compare the capacity of the new segmentation Spectralis OCT (Heidelberg Engineering, Inc., Heidelberg, Germany) prototype software to discriminate between healthy subjects and patients with suspected glaucoma. This capacity was also compared with that shown by the more conventional analysis of retinal nerve fibers at the peripapillary level. To the best of our knowledge, this is the first study to address the use of this new software in glaucoma suspects.

Methods

Thirty-eight glaucoma suspects and 38 age-matched healthy subjects were recruited from June 2013 to January 2014 for this

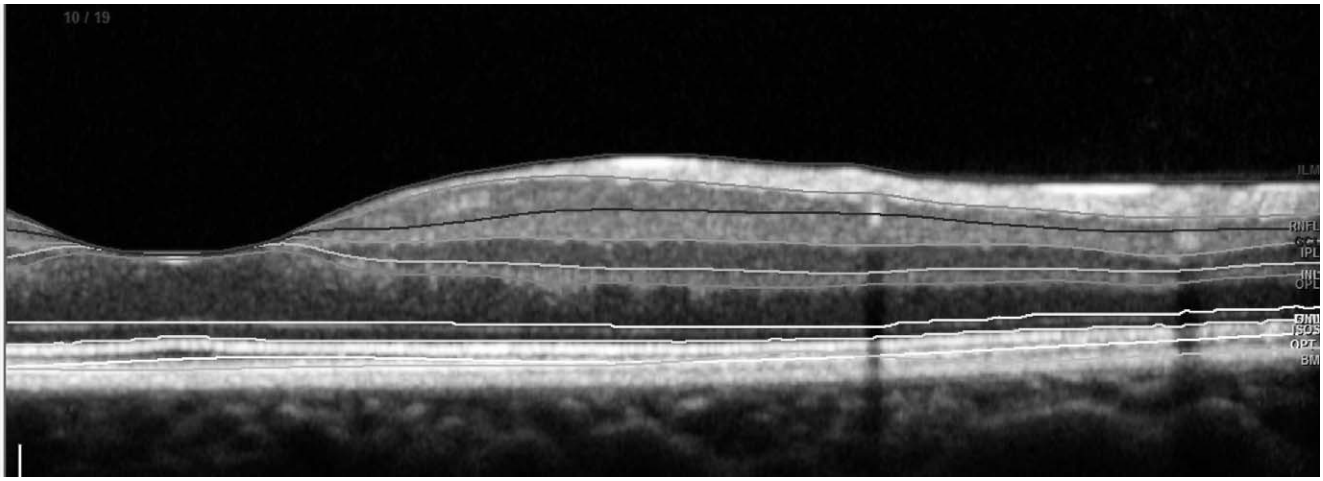

FIGURE 1. Retinal layer divisions determined using the new segmentation prototype software of the Spectralis OCT. The software automatically defines the retinal layers in a single horizontal foveal scan.

cross-sectional study. The study protocol received institutional review board approval and adhered to the tenets of the Declaration of Helsinki. Informed consent was obtained from all participants.

For both the patient and control groups, eligibility was determined after a complete ophthalmologic examination, including visual acuity, slit lamp examination of the anterior segment, IOP, a dilated fundus examination, and visual field testing using the Humphrey Visual Field Analyzer implementing a Swedish Interactive Threshold Algorithm Standard strategy (Carl Zeiss Meditec, Dublin, CA, USA). If fixation losses were greater than 20% or false-positive or false-negative rates were greater than 15%, the test was repeated. A normal standard automated perimetry (SAP) result was defined as visual field indices (mean deviation and pattern SD) within 95% confidence limits, with fewer than three nonedge contiguous points within the same hemifield identified as significant ($P < 0.05$) in the pattern deviation plot, and glaucomatous hemifield test results within normal limits.

All participants had to meet the following inclusion criteria: a best-corrected visual acuity of greater than 20/40, refractive error of less than 5 spherical diopters and 2 diopters of cylinder, transparent ocular media (nuclear color/opalescence, cortical or posterior subcapsular lens opacity <1) according to the Lens Opacities Classification System III system,[11] and an open anterior chamber angle. The exclusion criteria were having undergone intraocular surgery within 3 months before inclusion in the study, having diabetes, a history of eye or neurological disease, use of medication that could affect visual field sensitivity, and any disability, mental or other, that could prevent the correct understanding of the information needed for informed consent.

A glaucoma suspect was defined as showing a glaucomatous-appearing optic disc, an elevated IOP (>21 mm Hg), and a normal SAP result. A subject was classified as healthy if the appearance of the optic nerve disc was normal, IOP was lower than 21 mm Hg, and the SAP result was also normal.

When both eyes fulfilled the study's inclusion criteria, the data for only one randomly selected eye were entered in the analysis.

Optical Coherence Tomography

All subjects were examined using the "fast macular cube" and "RNFL" protocols of the Spectralis OCT.

Images were acquired using image alignment eye-tracking software (TruTrack; Heidelberg Engineering) to obtain perifoveal volumetric retinal scans comprising 25 single horizontal axial scans (scanning area: 666 mm^2 centered at the fovea). Segmentation of the retinal layers in single horizontal foveal scans was performed automatically using new prototype software for the Spectralis OCT (Fig. 1) to give the three measurements: RNFL, GCL, and GCC (GCL + inner plexiform layer). We selected the retinal thickness map analysis to display numeric averages of the measurements for each of nine subfields as defined by the Early Treatment Diabetic Retinopathy Study (ETDRS) (Fig. 2). The inner, intermediate, and outer rings of diameters 1, 3, and 6 mm, respectively, were considered for the analyses. The average of all points within the inner 1-mm radius circle was defined as central foveal thickness. The intermediate ring is divided into four zones designated as inner superior, inner nasal, inner inferior, and inner temporal; and the outer ring designated into outer superior, outer nasal, outer inferior, and outer temporal. The numerical values recorded for each of the nine zones were used in the analyses.

Peripapillary RNFL thickness measured around the disc in a circular 3.5-mm diameter 768 A-Scan was also determined in all subjects using the instrument's RNFL protocol. The RNFL thickness (from the inner margin of the internal limiting membrane to the outer margin of the RNFL layer) was automatically segmented using the Spectralis device software. Correction for fovea-disc orientation (FoDi) is incorporated in the software. While scanning with the FoDi software, an internal fixation point is provided for the subject. If the subject achieves foveal fixation, scan disc torsional status is guided by its intersection with the papillo-macular bundle. This intersection is considered the middle of the temporal sector. The superior, inferior, and nasal sectors are then consecutively arranged. In all cases, it was checked that foveal fixation was adequate.

An online tracking system was used to compensate for eye movements. The variables recorded were mean RNFL thicknesses in each of the six zones: superotemporal, superonasal, nasal, inferonasal, temporal, and inferotemporal. All scans were performed by the same experienced operator. No manual correction was applied to the OCT output. An internal fixation target was used to provide the highest reproducibility, as reported elsewhere.[12] The quality of the scans was assessed before analysis and poor-quality scans were rejected. The Spectralis OCT uses a blue quality bar in the image to indicate

Investigative Ophthalmology & Visual Science

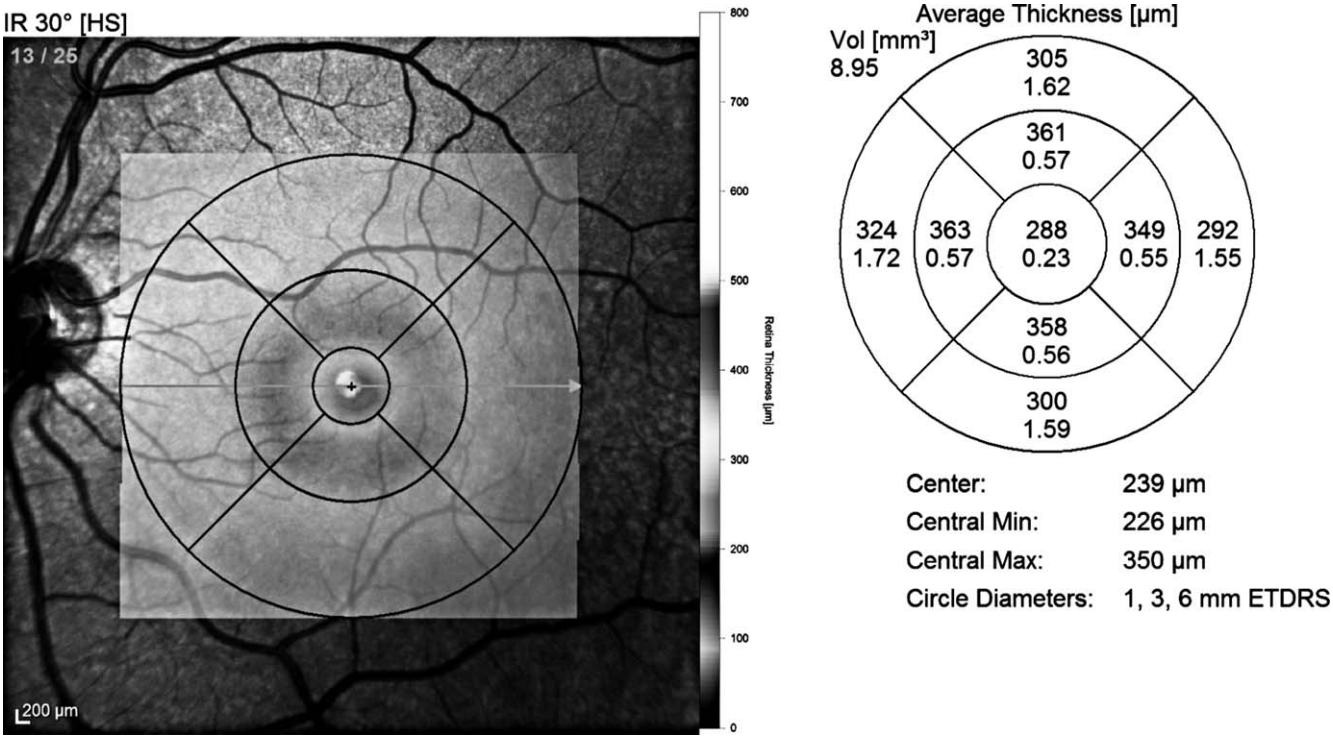

FIGURE 2. Retinal thickness analysis protocol showing mean thicknesses for each of nine ETDRS subfields.

signal strength. The quality score range is 0 (poor quality) to 40 (excellent quality). Only images scoring higher than 25 were included. The Spectralis software version used was 5.4b.

Statistical Analysis

Average mRNFL, GCL, GCC, and pRNFL thicknesses were compared between normal and glaucoma-suspect eyes using the Student's *t*-test for independent samples. The diagnostic capacity of each variable to differentiate between normal and glaucoma-suspect eyes was determined by calculating the area under the receiver operating characteristics (ROC) curve (AUC). The ROC curve shows the trade-off between sensitivity and specificity (false-positive rate). An AUC of 1.0 represents perfect discrimination, whereas an AUC of 0.5 represents chance discrimination. Differences between the ROC curves were tested to compare AUCs using the Hanley–McNeil method.[13] The sensitivity, specificity, positive predictive values, and negative predictive values of each variable varying significantly between the two subject groups were also calculated.

At least 33 patients had to be included in each group to detect a 4-µm difference in mRNFL thickness between groups for a statistical power of 80%, significance level of 5%, and assuming SDs of 5.9 and 5.6 mm Hg.[14] Thus, 40 patients were enrolled in each group, although two subjects per group had to be withdrawn due to segmentation artifacts in their OCT images, leaving a final study population of 38 individuals per group. All statistical tests were performed using SPSS version 21 (SPSS, Inc., Chicago, IL, USA) and MedCalc version 12.7 software (MedCalc software, Ostend, Belgium). Significance was set at P less than 0.05.

Results

Mean ages ± SD were 65.8 ± 13.6 years (range, 30–91) for the control subjects and 64.9 ± 12.0 years (range, 36–88) for the glaucoma suspects ($P = 0.742$). Mean visual field deviation was 0.05 ± 0.9 dB in the healthy subjects and 0.12 ± 1.4 dB in the glaucoma suspects ($P = 0.348$).

The mRNFL, pRNFL, GCL, and the GCC thickness measurements are provided in Table 1. Only the mRNFL measurements inner inferior ($P = 0.003$), outer inferior ($P = 0.017$), and inner temporal ($P = 0.010$) varied significantly between the two groups, with glaucoma suspects showing thinner values than the control subjects.

Sensitivities, specificities, positive and negative predictive values, and AUCs for the mRNFL, pRNFL, GCL, and GCC measurements are shown in Table 2. The variables featuring the larger AUCs were inner inferior (0.742), outer inferior (0.660), and inner temporal (0.651) mRNFL thicknesses. The best parameter for each of the other analyses were as follows: inner inferior GCL thickness (AUC = 0.559), inner temporal GCC thickness (0.529), and temporal pRNFL thickness (0.595) (Fig. 3). The AUC recorded for inner inferior mRNFL thickness was significantly higher than the areas obtained for the most discriminatory GCL (inner inferior, $P = 0.022$), GCC (inner temporal, $P = 0.004$), and pRNFL (temporal, $P = 0.042$) measurements (Table 3).

For the mRNFL thickness measurements, the cutoff offering best sensitivity (71.0%) and specificity (68.4%) in the inner inferior zone was 28 µm. This meant that eyes with an inner inferior mRNFL thickness below this value showed a 69.2% likelihood of incipient glaucoma (positive predictive value). In contrast, a patient with an inner inferior mRNFL thickness above this cutoff had a 70.3% probability of not having glaucoma (negative predictive value).

Discussion

In the field of glaucoma, interest in measuring macular thickness has recently mounted. The reason for this is that a high proportion of RGCs occur at the macula, and during

Table 1. Macular RNFL and pRNFL, GCC, and GCL Measurements (mean ± SD in μm) in Healthy Subjects and Patients With Suspected Glaucoma

Parameter	Control	Suspected Glaucoma	*P*
mRNFL			
Center	16.8 ± 6.8	14.8 ± 5.3	0.146
Inner superior	31.3 ± 4.0	30.1 ± 2.9	0.154
Inner nasal	26.3 ± 6.6	24.4 ± 2.4	0.109
Inner inferior	31.2 ± 7.6	27.2 ± 2.6	<0.001
Inner temporal	22.1 ± 2.1	21.1 ± 1.3	0.010
Outer superior	44.3 ± 5.5	42.2 ± 4.3	0.068
Outer nasal	46.1 ± 9.7	44.1 ± 6.9	0.292
Outer inferior	43.8 ± 6.0	40.8 ± 4.7	0.017
Outer temporal	26.0 ± 7.0	24.9 ± 6.0	0.451
GCC			
Center	37.0 ± 14.1	36.9 ± 12.0	0.972
Inner superior	96.1 ± 13.8	96.7 ± 7.8	0.807
Inner nasal	103.4 ± 20.6	100.8 ± 14.0	0.532
Inner inferior	98.4 ± 16.1	95.0 ± 14.5	0.342
Inner temporal	90.7 ± 10.5	89.7 ± 11.9	0.714
Outer superior	62.3 ± 7.0	62.9 ± 7.7	0.708
Outer nasal	78.1 ± 10.4	79.5 ± 9.3	0.540
Outer inferior	63.9 ± 7.8	64.7 ± 8.7	0.668
Outer temporal	73.3 ± 8.0	73.8 ± 9.8	0.818
GCL			
Center	16.7 ± 8.0	17.2 ± 6.7	0.756
Inner superior	55.4 ± 8.1	55.5 ± 7.0	0.964
Inner nasal	56.8 ± 9.9	57.6 ± 8.6	0.711
Inner inferior	56.3 ± 8.8	54.0 ± 9.2	0.275
Inner temporal	49.9 ± 10.4	50.8 ± 8.5	0.665
Outer superior	28.6 ± 5.5	30.5 ± 10.7	0.342
Outer nasal	38.9 ± 5.2	40.7 ± 5.8	0.143
Outer inferior	30.1 ± 3.7	29.7 ± 4.5	0.657
Outer temporal	34.8 ± 6.1	33.7 ± 6.0	0.454
pRNFL			
Global	100.0 ± 9.6	99.1 ± 10.6	0.701
Superotemporal	133.4 ± 22.3	140.0 ± 50.3	0.464
Superonasal	104.0 ± 18.9	99.1 ± 25.7	0.342
Nasal	76.6 ± 11.5	76.6 ± 15.3	0.980
Inferonasal	122.6 ± 22.7	123.5 ± 24.0	0.868
Inferotemporal	143.8 ± 21.5	141.8 ± 17.8	0.664
Temporal	72.5 ± 10.9	68.7 ± 9.5	0.111

glaucoma progression this could determine macular thinning. However, macular thickness has not proved to be a reliable prognostic marker of glaucoma and is also affected by other diseases involving the central retinal zone, whose prevalence, as for glaucoma, increases with age. This has meant that overall macular thickness measurements are no longer a component of the diagnosis of glaucoma.

Ishikawa et al.[15] developed a prototype software package to selectively analyze the internal retinal layers based on images obtained through time-domain OCT. These authors showed that inner retinal measurements offered a similar diagnostic power to the study of the peripapillary nerve fiber layer in terms of discriminating between patients with glaucoma and healthy controls. This diagnostic capacity also was improved over that of overall macular thickness. Subsequent to this, Tan et al.[16] obtained similar results in glaucoma suspects. However, the limited resolution of time-domain OCT prevented any further advances in this type of analysis.

Developments in this field have led to a high reproducibility of morphometric macular measurements using spectral-domain OCT, which offers improved resolution over the time-domain technique. Many OCT instruments currently on the market allow for a detailed study of the different macular layers, although, depending on the model, segmentation of the different layers is differently achieved. Thus, the Cirrus OCT (Carl Zeiss Meditec) examines the ganglion cell layer together with the internal plexiform layer, and the RTVUE OCT (Optovue, Inc., Fremont, CA, USA) analyzes the whole GCC (GCL + internal plexiform layer + RNFL). Using software presently under development, the Spectralis OCT conducts measurements individually on each of the three layers of the complex. To date, however, this type of ganglion cell analysis has not shown an improved diagnostic capacity over the study of the RNFL at the peripapillary level.[17–19]

In the present study, we observed that using the new macular segmentation software of the Spectralis OCT, nerve fiber layer thickness measurements at the level of the macula performed better than the other algorithms to discriminate between healthy subjects and glaucoma suspects. These findings are consistent with the observations made by Kotera et al.,[14] who, using the Topcon 3D-OCT-1000 (Topcon Corp., Tokyo, Japan) also detected differences between healthy subjects and glaucoma suspects in some zones of the macular RNFL. However, similar differences also were found in thickness measurements such as RNFL + GCL + inner plexiform layer, overall macular thickness, and pRNFL. These differences between the two studies could be related to the fact that the Topcon OCT semiautomatically delineates the macular layers and the border between the internal plexiform and internal nuclear layers is manually defined, whereas the Spectralis OCT automatically defines the different layers using an algorithm. Differences in axial resolution and image capture velocity (27,000 vs 40,000 A-scans/s) also may explain the different findings of the two studies.

Using the FoDi alignment software of the Spectralis OCT, it can be checked that foveal fixation of the individual under test is adequate. There is currently much controversy over the repercussions on RNFL thickness measurements of scan disc torsion during image acquisition. In the present study, an internal fixation point in the device was used and the correct foveal fixation of the subject was verified. All individuals

Table 2. Diagnostic Performance of mRNFL and pRNFL, GCC, and GCL Measurements

	Best Cutoff	Sensitivity, %	Specificity, %	+LR	−LR	PPV, %	NPV, %	AUC	Sp 80%, %	Sp 90%, %
mRNFL inner inferior	<28	71.0	68.4	2.25	0.42	69.2	70.3	0.742	51.7	24.9
mRNFL outer inferior	<40	52.6	76.3	2.22	0.62	69.0	61.0	0.660	46.0	22.4
mRNFL inner temporal	<21	68.4	55.3	1.53	0.57	60.5	63.6	0.651	37.6	11.0
GCL inner Inferior	<59	76.3	42.1	1.32	0.56	56.9	64.0	0.559	22.0	14.3
GCC inner temporal	≤89	57.9	52.6	1.22	0.8	55.0	55.6	0.529	21.9	8.9
pRNFL temporal	≤69	65.8	57.9	1.56	0.59	61.0	62.9	0.595	23.7	16.9

+LR, positive likelihood ratio; −LR, negative likelihood ratio; PPV, positive predictive value; NPV, negative predictive value; Sp 80%, sensitivity for a specificity fixed at 80%; Sp 90%, sensitivity for a specificity fixed at 90%.

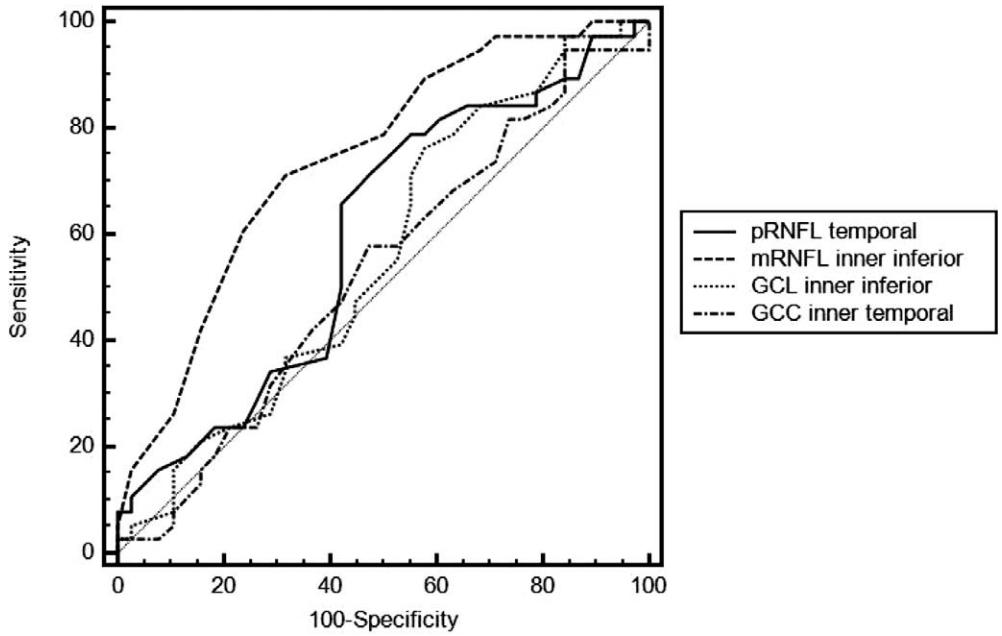

FIGURE 3. Receiver operating characteristic curves for the variables showing the best discriminant capacity between the two subject groups; AUC: 0.742 mRNFL inner inferior, 0.595 pRNFL temporal, 0.559 GCL inner inferior, and 0.529 GCC inner temporal.

showed adequate foveal fixation so that subsequent image modification was not required. In this way, we can avoid possible examiner effects when acquiring data.

The present data seem to indicate that the first detectable changes produced at the initial stages of glaucoma occur at the level of the macular nerve fiber layer containing the ganglion cell axons. In contrast, modifications in the layer containing the ganglion cell bodies and the internal plexiform layer containing dendrites seem to occur at a later stage. This rationale is in agreement with histological findings that indicate that most cell body death occurs after axon degeneration.[20–23] However, these findings need to be confirmed in longitudinal studies designed to confirm the timing of these events. Given that our study was cross-sectional, we cannot really be sure which layer will be first affected nor if all patients included as glaucoma suspects with mRNFL alterations will eventually develop glaucoma. The present lack of a normative database for the prototype software used means it is unknown in which percentage of patients the mRNFL will be already affected when GCL or GCC measurements are still within the normal range.

The topography of the defects observed here is also consistent with the information available in the literature. At the level of the pRNFL, the superior and inferior zones showed best diagnostic performance. At the macular level, defects also were detected in these zones such that the variables returning significantly greater areas under the ROC curve were inner inferior and outer inferior mRNFL thickness.

TABLE 3. Comparing the Measurements Showing the Best Discriminant Capacity With the Best mRNFL Measurement

	Difference in AUC Versus Outer Inferior mRNFL	*P*
GCL inner inferior	0.183	0.022
GCC inner temporal	0.212	0.004
pRNFL temporal	0.147	0.042

In conclusion, our findings indicate that macular RNFL thickness shows an improved capacity to discriminate between healthy subjects and glaucoma suspects over that shown by other inner retinal layer measurements. The macular nerve fiber layer thickness differences detected between the two groups of subjects could reflect the axon degeneration that occurs during the course of glaucoma. This degeneration will subsequently lead to retinal ganglion cell death.

Acknowledgments

Supported in part by Instituto de Salud Carlos III, "Red temática de Investigación Cooperativa, Proyecto RD07/0062: Patología ocular del envejecimiento, calidad visual y calidad de vida" and Grupo de Investigación de la Universidad Complutense de Madrid 920415-GR58/08. The authors alone are responsible for the content and the writing of the paper.

Disclosure: **J.M. Martinez-de-la-Casa**, None; **P. Cifuentes-Canorea**, None; **C. Berrozpe**, None; **M. Sastre**, None; **V. Polo**, None; **J. Moreno-Montañes**, None; **J. Garcia-Feijoo**, None

References

1. American Academy of Ophthalmology Glaucoma Panel. *Preferred Practice Pattern. Primary Open-Angle Glaucoma*. San Francisco, CA: American Academy of Ophthalmology; 2005:3.
2. Quigley HA. Neuronal death in glaucoma. *Prog Retin Eye Res*. 1999;18:39–57.
3. Weinreb RN, Khaw PT. Primary open-angle glaucoma. *Lancet*. 2004;363:1711–1720.
4. Spaeth G, Walt J, Keener J. Evaluation of quality of life for patients with glaucoma. *Am J Ophthalmol*. 2006;141:3–14.
5. Parrish RK II, Schiffman JC, Feuer WJ, et al. Ocular Hypertension Treatment Study Group. Test-retest reproducibility of optic disk deterioration detected from stereophotographs by masked graders. *Am J Ophthalmol*. 2005;140:762–764.
6. Zeyen T, Miglior S, Pfeiffer N, Cunha-Vaz J, Adamsons I. European Glaucoma Prevention Study Group. Reproducibility

of evaluation of optic disc change for glaucoma with stereo optic disc photographs. *Ophthalmology*. 2003;110:340–344.

7. Zeimer R, Asrani S, Zou S, Quigley H, Jampel H. Quantitative detection of glaucomatous damage at the posterior pole by retinal thickness mapping: a pilot study. *Ophthalmology*. 1998;105:224–231.
8. Bagga H, Greenfield DS, Knighton RW. Macular symmetry testing for glaucoma detection. *J Glaucoma*. 2005;14:358–363.
9. Wollstein G, Schuman JS, Price LL, et al. Optical coherence tomography (OCT) macular and peripapillary retinal nerve fiber layer measurements and automated visual fields. *Am J Ophthalmol*. 2004;138:218–225.
10. Lederer DE, Schuman JS, Hertzmark E, et al. Analysis of macular volume in normal and glaucomatous eyes using optical coherence tomography. *Am J Ophthalmol*. 2003;135:838–843.
11. Chylack LT Jr, Wolfe JK, Singer DM, et al. The Lens Opacities Classification System III. *Arch Ophthalmol*. 1993;111:831–836.
12. Schuman JS, Pedut-Kloizman T, Hertzmark E, et al. Reproducibility of nerve fiber layer thickness measurements using optical coherence tomography. *Ophthalmology*. 1996;103:1889–1898.
13. Hanley JA, McNeil BJ. A method of comparing the areas under receiver operating characteristic curves derived from the same cases. *Radiology*. 1983;148:839–843.
14. Kotera Y, Hangai M, Hirose F, Mori S, Yoshimura N. Three-dimensional imaging of macular inner structures in glaucoma by using spectral-domain optical coherence tomography. *Invest Ophthalmol Vis Sci*. 2011;52:1412–1421.
15. Ishikawa H, Stein DM, Wollstein G, Beaton S, Fujimoto JG, Shuman JS. Macular segmentation with optical coherence tomography. *Invest Ophthalmol Vis Sci*. 2005;46:2012–2017.
16. Tan O, Li G, Lu AT, Varma R, Huang D. Advanced imaging for glaucoma study group. Mapping of macular substructures with optical coherence tomography for glaucoma diagnosis. *Ophthalmology*. 2008;115:949–956.
17. Francoz M, Fenolland JR, Giraud JM, et al. Reproducibility of macular ganglion cell-inner plexiform layer thickness measurement with cirrus HD-OCT in normal, hypertensive and glaucomatous eyes. *Br J Ophthalmol*. 2014;98:322–328.
18. Tan O, Chopra V, Lu AT, et al. Detection of macular ganglion cell loss in glaucoma by Fourier-domain optical coherence tomography. *Ophthalmology*. 2009;116:2305–2314.
19. Seong M, Sung KR, Choi EH, et al. Macular and peripapillary retinal nerve fiber layer measurements by spectral domain optical coherence tomography in normal-tension glaucoma. *Invest Ophthalmol Vis Sci*. 2010;51:1446–1452.
20. Morrison JC, Dorman-Pease ME, Dunkelberger GR, Quigley HA. Optic nerve head extracellular matrix in primary optic atrophy and experimental glaucoma. *Arch Ophthalmol*. 1990;108:1020–1024.
21. Quigley HA, Brown A, Dorman-Pease ME. Alterations in elastin of the optic nerve head in human and experimental glaucoma. *Br J Ophthalmol*. 1991;75:552–557.
22. Quigley HA, Addicks EM. Chronic experimental glaucoma in primates II. Effect of extended intraocular pressure elevation on optic nerve head and axonal transport. *Invest Ophthalmol Vis Sci*. 1980;19:137–152.
23. Martin KR, Quigley HA, Valenta D, Kielczewski J, Pease ME. Optic nerve dynein motor protein distribution changes with intraocular pressure elevation in a rat model of glaucoma. *Exp Eye Res*. 2006;83:255–262.

Investigative Ophthalmology & Visual Science